Challenge Journal of Structural Mechanics

Research Article

Numerical investigation of the effect of minaret height on its dynamic characteristics

Hakan Erkek [a], Musa Yetkin [b,*], İbrahim Özgür Dedeoğlu [c]

[a] *Department of Civil Engineering, Osmaniye Korkut Ata University, 80010 Osmaniye, Türkiye*
[b] *Department of Civil Engineering, Fırat University, 23119 Elazığ, Türkiye*
[c] *Department of Civil Engineering, Batman University, 72000 Batman, Türkiye*

ABSTRACT

Minarets are structures that have an important place in Islamic architecture. Although these structures have a long, thin and delicate appearance, they can be constructed in different cross-sections and heights. Due to their geometry, minarets can be damaged under earthquake and wind loads. In order to minimize the possibility of damage to these structures, they must be constructed with suitable geometry and materials. In this study, the effect of minaret height on dynamic characteristics (natural frequency and mode shape) was investigated numerically. For numerical application, 19 different minarets with heights ranging from 13.5 m to 33.75 m were modeled in the ANSYS finite element package program. It is assumed that the minarets have as masonry and the base of the minaret was fixed support to the soil. These minarets were evaluated in terms of natural frequency, mode shape and modal mass participation ratios by performing modal analyses. In addition, an equation has been derived that can predict the first natural frequency of the minaret depending on its height.

ARTICLE INFO

Article history:
Received 8 November 2022
Revised 7 December 2022
Accepted 20 December 2022

Keywords:
Minaret
Dynamic characteristic
Natural frequency
Mode shape
Modal mass participation ratio

1. Introduction

Minarets are tower-shaped tall structures built for the purpose of chanting the call to prayer and spreading the sound around. These structures, which are built adjacent to or separately from mosques, have one or more balconies, and the doors of these balconies must face to the qibla. In minarets built adjacent to the mosque, the minaret entrance door usually opens into the mosque. Minarets of different geometries and heights have been built and are still being built all over the world. The minaret of the II. Hasan Mosque in Morocco is the tallest minaret in the world (with a height of 210 m), and the minaret of the Sabancı Merkez Mosque in Adana is the highest minaret in Türkiye (with a height of 99 m) (Fig. 1).

Minarets, which have an important place in Islamic architecture, carry traces of the time they were built and are symbolic structures that have an important place in the urban fabric. Minarets built in different regions reflect the culture of the region they were built because they have different identities. For example, Seljuk and Syrian minarets are generally short, while Ottoman minarets are longer. Iraqi minarets are generally cone-shaped, while Arab minarets are rectangular. In Egyptian architecture, minarets are usually square at the bottom, octagonal in the middle and dome-shaped at the top. Moroccan-style minarets are square at the base as in Egyptian architecture, and as the minaret height increases, narrowing is seen in the section.

Minarets are mostly built with a carcass and masonry load bearing system. While carcass minarets are generally made of reinforced concrete, wood and steel materials, masonry minarets are generally made of stone and brick materials. Minarets are built using these building materials in a way that consists of seven different parts. Minaret parts are boot (pulpit), transition segment, body, balcony, upper part of the minaret body, spire and end ornament. In addition, there are stairs built with or

* *Corresponding author*. Tel.: +90-424-237-0000 ; Fax: +90-424-241-5526 ; E-mail address: musayetkin@firat.edu.tr (M. Yetkin)
ISSN: 2149-8024 / DOI: https://doi.org/10.20528/cjsmec.2023.01.003

without a core inside the minarets, and these stairs generally continue up to the upper part of the minaret body. Explanations about the minaret parts are given below:

- The boot (pulpit) is the bottom part of the minaret, adjacent to the soil/foundation. This part can usually be built as rectangular, cylindrical and polygonal, and in minarets built separately from the mosque, the minaret door is mostly located in this part.
- The transition segment is the part that connects the boot and the body parts. This part is not encountered in minarets that do not differ in size and geometry between the boot and the body.
- The body is the part between the transition segment and the balcony and is generally cylindrical. In order to provide lighting and ventilation in the minaret, small windows are usually opened at regular intervals in this part.
- The balcony is one of the most aesthetically striking parts of the minarets. Almost every minaret has at least one balcony, and in some minarets it is possible to come across 3 balconies.
- The upper part of the minaret body is the part between the balcony and the spire, and is usually built with the same cross-section as the body part.
- The spire is the part that can be called the roof of the minarets and is generally built in the form of cones and domes.
- The end ornament is the part on the top of the minaret that is made in various ways to add beauty to the shape of the spire.

a) II. Hasan Mosque (Morocco) b) Sabancı Merkez Mosque

Fig. 1. The tallest minarets of the (a) world and (b) Türkiye.

Minarets can be damaged or collapsed under earthquake and wind forces due to the structural factors revealed by their architectural appearance (Fig. 2). Various studies are carried out by researchers in order to understand the reasons for these negative situations, to identify minarets that may have the potential to be damaged/collapsed, and to determine what precautions can be taken for minarets with this potential.

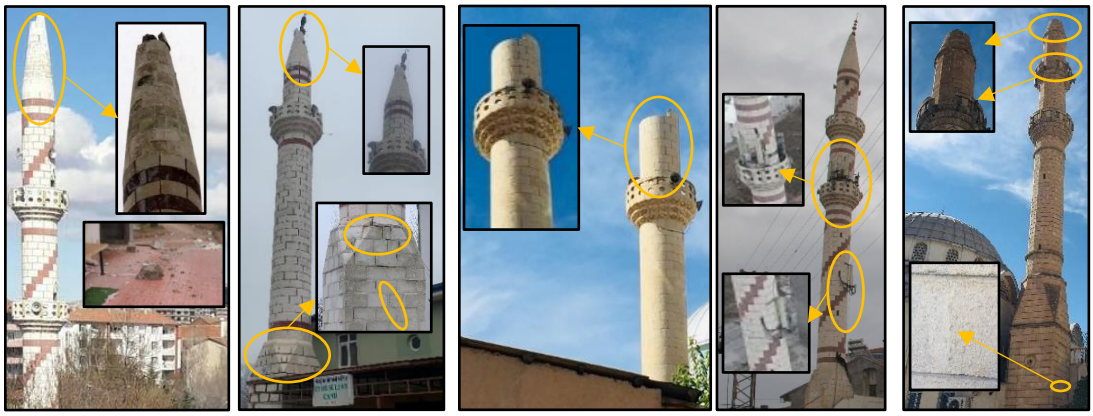

Fig. 2. Some examples for minaret damages (Yetkin et al. 2021).

Köksal et al. (2016) determined the dynamic behavior of the masonry minaret of the Yörgüç Pasha mosque (Samsun) against the ground motion caused by the surface blast-induced ground motion artificially generated

for the finite element model they created. Döven et al. (2018) modeled the Kütahya Yeşil Mosque minaret in two different ways as open and closed balconies, and then performed the experimental measurements of the minaret using operational modal analysis method using 2 different types of accelerometers and compared the finite element model analysis results they obtained with the experimental results. Yetkin et al. (2018) experimentally determined the dynamic characteristics of a reinforced concrete minaret and updated the finite element model in the light of these values. Adam et al. (2020) created a finite element model of a historical masonry minaret and determined its structural behavior under various loadings. Bayraktar and Hökelekli (2020) performed modal analyses and nonlinear seismic performance analyses of different types of minaret-foundation-soil interaction systems for different foundation types. Bayraktar and Hökelekli (2021) created finite element models for minaret types, which they assumed to be formed with different materials, and performed nonlinear analyses by strengthening these models with various methods. At the end of the study, they proposed a cost-effective seismic reinforcement technique with better workability and lower cost. Calayir et al. (2021) updated the finite element model of a masonry minaret by using the dynamic characteristics obtained from the operational modal analysis. Yetkin et al. (2021a) after the M_w=6.8 earthquake that occurred in Elazığ on January 24, 2020, they determined the damages in the minarets in the province of Elazığ and evaluated the causes of these damages. At the end of the study, they made some recommendations for the repair and strengthening of existing damaged minarets and the construction of new minarets. Yetkin et al. (2021b) carried out experimental measurements for a reinforced concrete minaret and updated the numerically constructed finite element model by taking into account the minaret-foundation-soil interaction using the shape functions/mode shapes they obtained. Yetkin et al. (2021c) determined the dynamic characteristics of a reinforced concrete minaret based on environmental vibration data for different measurement schemes. Usta (2021) created finite element models of five different minarets and determined their seismic behavior under various earthquakes. Yurdakul et al. (2021) investigated the earthquake performance of a historical masonry minaret. As a result of finite element model analysis, they stated that damages may occur in some parts of the minaret body.

Although there is no comprehensive standard for minaret design today, there is only a guide published by Presidency of the Republic of Türkiye Presidency of Religious Affairs (PRTPRA) in 2021, which sets some standards on minaret geometry. In this study, finite element models of 19 different masonry minarets with different heights were created, taking into account the guideline published by the PRTPRA. Then, modal analyses were performed for these models. The natural frequencies, mode shapes and modal mass participation ratios obtained as a result of the analyses were evaluated by comparing them with each other. In addition, an equation has been derived to predict the first natural frequency of the minaret depending on the minaret height.

2. Material and Method

2.1. Mosque planning and design guide

The Mosque Planning and Design Guide - 2021 (MPDG 2021), which is recommended to be used in new mosques by the PRTPRA has been published. This guide has brought new recommendations for mosque construction in many respects. Some of these recommendations were made for the design of minarets. These recommendations can be listed as a number of ratios in terms of the numbers and locations of minarets, the number of balconies, the dimensions of the balcony parapets, the width dimensions of the stairs, the positions of the minaret entrance doors and balconies, and the height between the minaret parts according to the mosque type. Some recommendations regarding minaret geometry are given in Fig. 3.

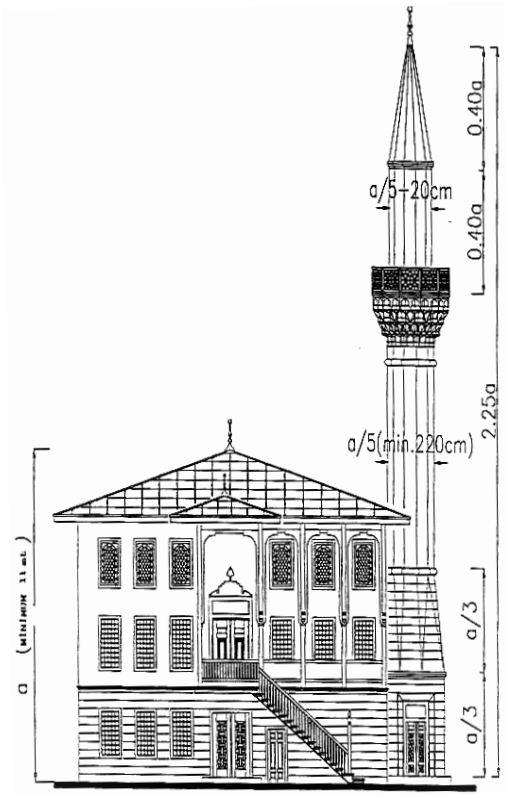

Fig. 3. Some recommendations on minaret geometry (MPDG 2021).

Within the scope of this study, the effect of height variation on natural frequencies, mode shapes and modal mass participation ratios is investigated for minarets with different heights, considering the relationships given in Fig. 3.

3. Numerical Application

Within the scope of the study, finite element models were created by choosing minarets with different heights. While choosing the geometry of each parts of the minarets, the recommendations given in MPDG (2021)

were followed (Fig. 3). The minarets created consist of a single balcony. Door openings at the entrance and balcony of the minarets were taken into account. Details of minaret geometries are given in Table 1.

Table 1. Details of minaret geometries.

*a** (m)	Boot height (m)	Transition segment height (m)	Body (m)	Upper part of the minaret body height (m)	Spire (m)	Wall thickness (m)	Boot cross-section (m^2)	Cylindrical outer diameter (m)	Door openings (m^2)	Total height (m)
6.0	2.00	2.00	4.70	2.40	2.40					13.500
6.5	2.17	2.17	5.09	2.60	2.60					14.625
7.0	2.33	2.33	5.48	2.80	2.80					15.750
7.5	2.50	2.50	5.87	3.00	3.00					16.875
8.0	2.67	2.67	6.27	3.20	3.20					18.000
8.5	2.83	2.83	6.66	3.40	3.40					19.125
9.0	3.00	3.00	7.05	3.60	3.60					20.250
9.5	3.17	3.17	7.44	3.80	3.80					21.375
10.0	3.33	3.33	7.83	4.00	4.00					22.500
10.5	3.50	3.50	8.22	4.20	4.20	0.25	2.6×2.6	2.2	0.5×1.7	23.625
11.0	3.67	3.67	8.62	4.40	4.40					24.750
11.5	3.83	3.83	9.01	4.60	4.60					25.875
12.0	4.00	4.00	9.40	4.80	4.80					27.000
12.5	4.17	4.17	9.79	5.00	5.00					28.125
13.0	4.33	4.33	10.18	5.20	5.20					29.250
13.5	4.50	4.50	10.57	5.40	5.40					30.375
14.0	4.67	4.67	10.97	5.60	5.60					31.500
14.5	4.83	4.83	11.36	5.80	5.80					32.625
15.0	5.00	5.00	11.75	6.00	6.00					33.750

* *a* parameter is given in Fig. 3.

It has been accepted that the minarets have a masonry load bearing system. In the finite element modelling, macro modelling approach was used, and the elasticity modulus, density and Poisson's ratio of the masonry material were chosen as 14000 MPa, 2200 kg/m^3 and 0.2, respectively. It has assumed that the minarets are fixed support at the foundation level. All modellings and analyses were performed with the ANSYS package program (ANSYS 2009). An example of the finite element modelling of minarets is given in Fig. 4.

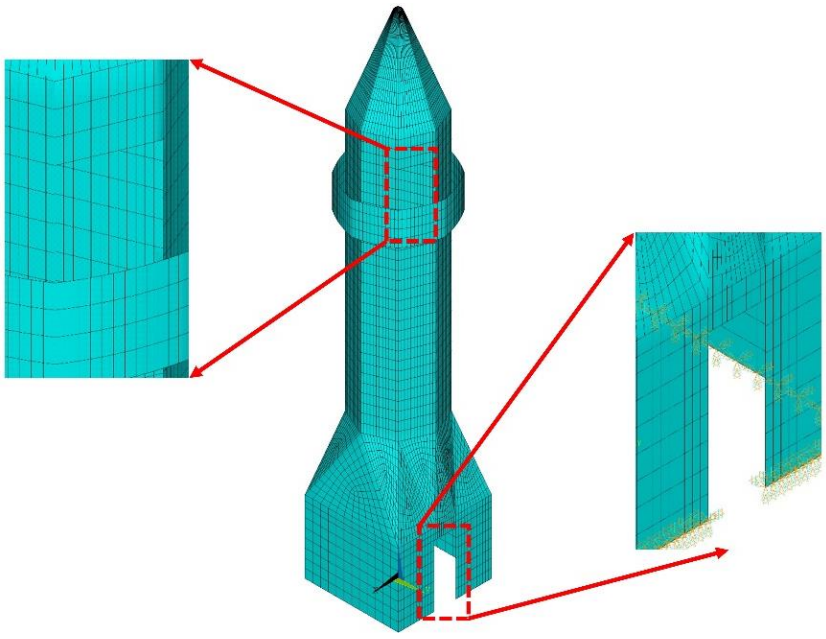

Fig. 4. An example of the finite element modelling of minarets.

4. Results and Discussion

The modal analyses were performed for all minarets and the first 10 natural frequency values obtained are presented in Table 2. When the natural frequency values are examined, it is seen that the natural frequency value decreases as the minaret height increases (the case of the a parameter increasing from 6.0 to 15.0). The largest decrease was 82.56% for the 1st natural frequency value and the smallest decrease was 58.01% for the 5th natural frequency value (Fig. 5).

An equation was derived that allows the first natural frequency values obtained from the study to be estimated depending on the a parameter (Eq. (1)). For Eq. (1), f_1 denotes the first natural frequency value (Hz) and a denotes the parameter related to height (m) shown in Fig. 3.

$$f_1 = 4.229a^4\ x\ 10^{-5} - 2.147a^3\ x\ 10^{-3} + 4.181a^2\ x\ 10^{-2} - 3.799a\ x\ 10^{-1} + 1.44 \quad (1)$$

Table 2. Natural frequency values for the first 10 modes of minarets (in Hz).

Mode	a parameter values (m)																		
	6.0	6.5	7.0	7.5	8.0	8.5	9.0	9.5	10.0	10.5	11.0	11.5	12.0	12.5	13.0	13.5	14.0	14.5	15.0
1	0.258	0.223	0.194	0.171	0.151	0.135	0.121	0.109	0.099	0.090	0.082	0.076	0.070	0.064	0.060	0.055	0.052	0.048	0.045
2	0.262	0.226	0.197	0.173	0.154	0.137	0.123	0.111	0.100	0.091	0.084	0.077	0.071	0.065	0.060	0.056	0.052	0.049	0.046
3	1.092	0.968	0.862	0.771	0.693	0.625	0.566	0.515	0.471	0.432	0.397	0.366	0.339	0.315	0.293	0.273	0.255	0.239	0.224
4	1.112	0.980	0.870	0.777	0.699	0.632	0.574	0.523	0.478	0.439	0.404	0.373	0.345	0.321	0.298	0.278	0.260	0.244	0.229
5	1.196	1.110	1.036	0.971	0.914	0.864	0.818	0.778	0.741	0.707	0.677	0.649	0.623	0.599	0.577	0.556	0.537	0.519	0.502
6	1.624	1.511	1.411	1.324	1.247	1.178	1.115	1.059	1.006	0.949	0.884	0.822	0.766	0.715	0.669	0.627	0.589	0.554	0.522
7	2.225	1.990	1.790	1.618	1.470	1.340	1.227	1.128	1.042	0.974	0.912	0.848	0.789	0.737	0.689	0.645	0.606	0.570	0.537
8	2.281	2.040	1.835	1.659	1.507	1.375	1.259	1.156	1.066	0.985	0.927	0.887	0.850	0.817	0.787	0.758	0.732	0.707	0.684
9	3.111	2.881	2.684	2.512	2.361	2.225	2.090	1.936	1.793	1.664	1.549	1.445	1.351	1.266	1.188	1.118	1.053	0.993	0.938
10	3.723	3.342	3.017	2.738	2.497	2.288	2.115	1.969	1.824	1.692	1.573	1.466	1.369	1.281	1.201	1.128	1.062	1.000	0.944

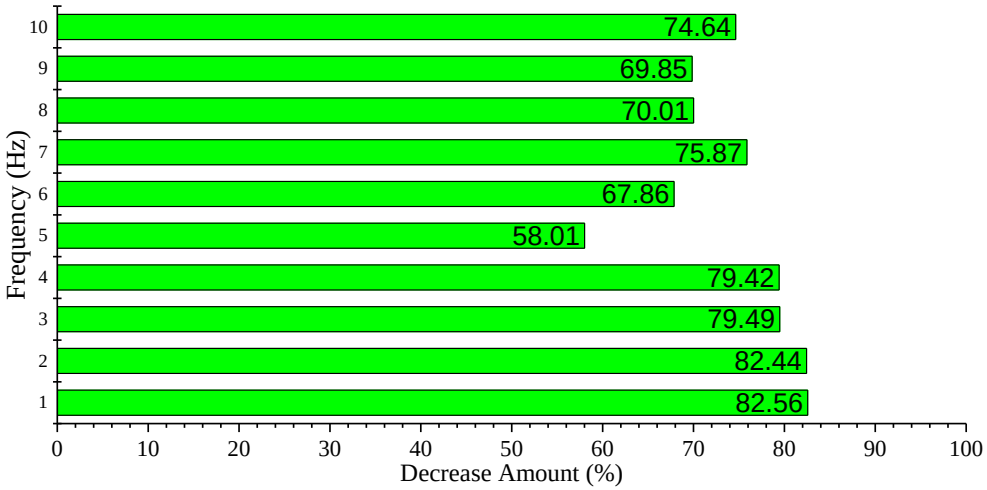

Fig. 5. The decrease amount in the natural frequency for the case where the a parameter increases from 6 to 15.

As a result of the modal analyses of the minarets, the mode shapes were obtained also. It has been observed that the mode shapes are generally similar. For this reason, mode shapes for only a=6.0 m solutions are given for the first 10 modes (Fig. 6). Graphics of visual comparison of mode shapes from different perspectives are shown in Figs. 7 and 8. According to Figs. 7 and 8, it is possible to say that the similarity of mode shapes is higher for the first modes, but this similarity gradually decreases for the later modes.

Furthermore, modal mass participation ratios (MMPR) were calculated as a result of the modal analysis of the minarets. In order to evaluate the effect of each mode on this ratio in a wider perspective, the MMPR of the first 50 modes are calculated and given in Tables 3 and 4.

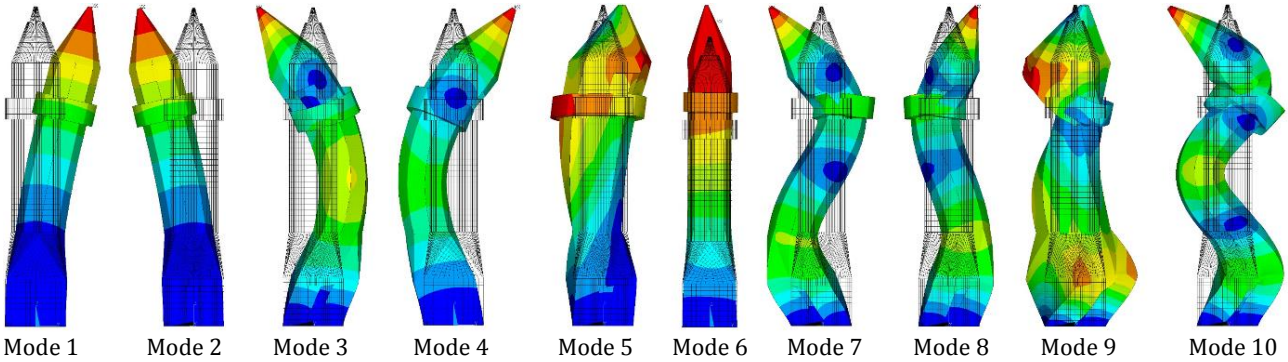

Fig. 6. First 10 mode shapes for a=6.0 m solutions.

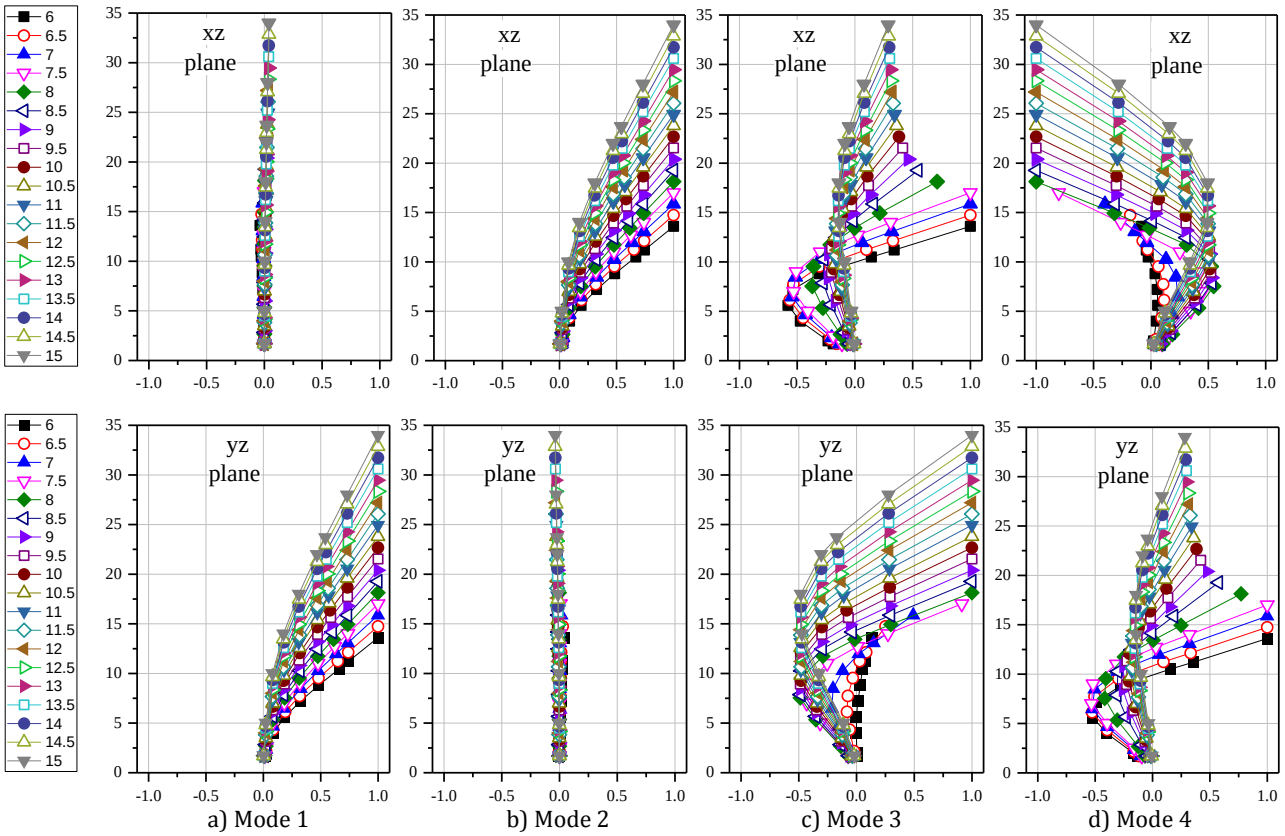

Fig. 7. Comparisons of mode shapes 1-4.

For the MMPR values given in Tables 3 and 4, values between 86.701-89.970% in the x direction and 81.996-85.225% in the y direction were obtained for the first 10 modes. For the first 10 modes, it was observed that as the minaret height increased, the MMPR decreased for both directions (x-y). For the first 20 and first 30 modes, there is no such relationship between minaret height and the MMPR. For the first 40 modes, values in the range of 94.056-96.532% in the x direction and 94.016-96.344% in the y direction were obtained. For the first 50 modes, values in the range of 94.859-96.827% in the x direction and 94.703-96.750% in the y direction were obtained. For the first 40 and 50 modes, the MMPR increased as the minaret height increased.

5. Conclusions

In this study, the effect of height on dynamic characteristics was investigated for 19 different minaret examples with heights ranging from 13.5 to 33.75 m. Finite element models of these 19 different minarets were created for numerical application. It is assumed that the minarets were built as masonry and connected to the soil with a fixed support. In addition, it is thought that the minarets have only one balcony, and both the balcony and the minaret entrance door openings are taken into account. Modal analyses were carried out for the minarets and their evaluations were made in terms of natural frequencies, mode shapes and modal mass participation ratios. The results obtained within the scope of the study are listed below:

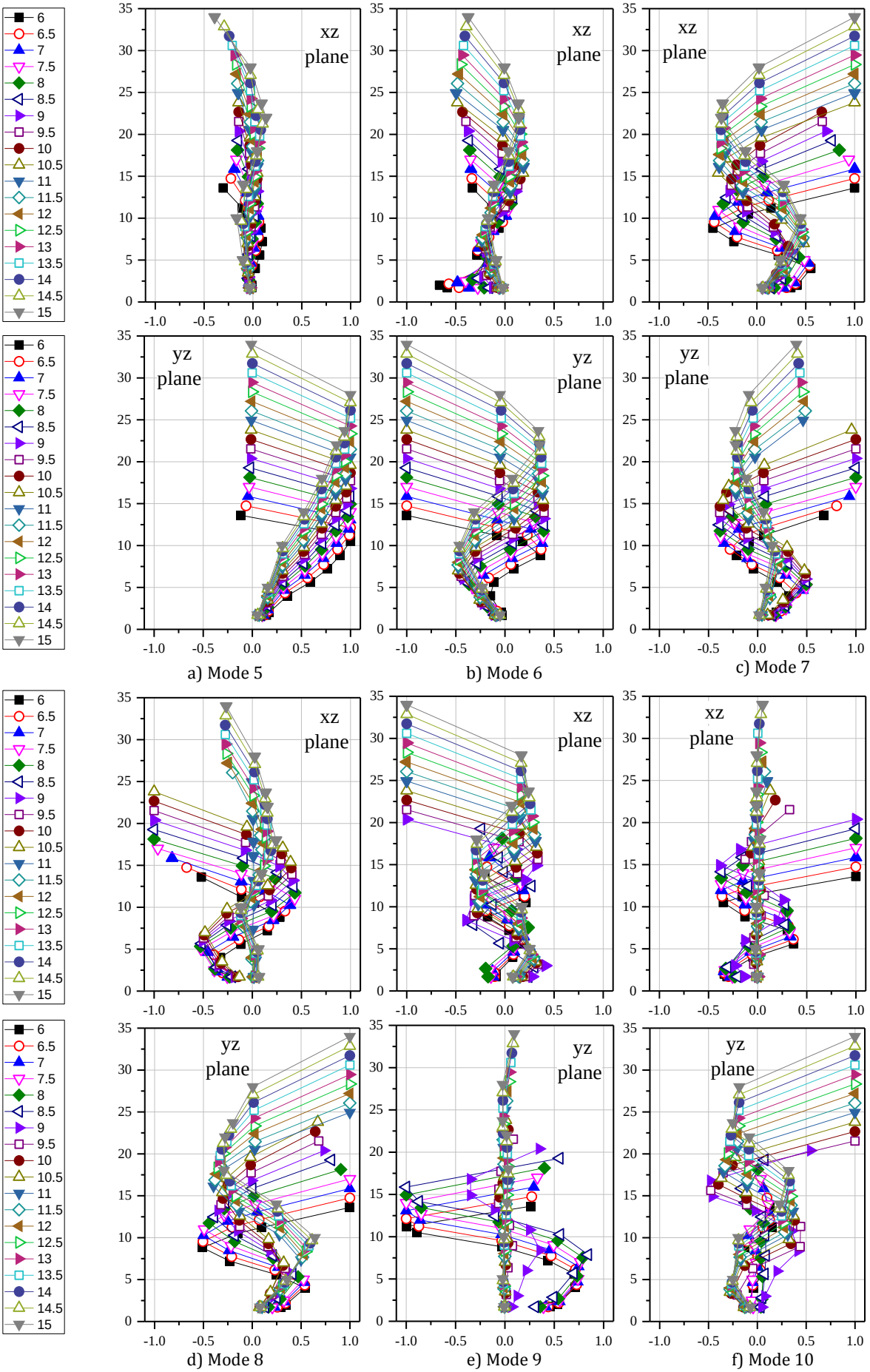

Fig. 8. Comparisons of mode shapes 5-10.

Table 3. Modal mass participation ratios (MMPR) for the *x* direction.

Mode	α parameter values (m)															
	6.0	6.5	7.0	7.5	8.0	8.5	9.0	9.5	10.0	10.5	11.0	11.5	12.0	12.5	13.0	13.5	14.0	14.5	15.0
1	0.077	0.032	0.010	0.001	0.001	0.005	0.011	0.019	0.026	0.033	0.040	0.046	0.051	0.056	0.060	0.064	0.067	0.070	0.072
2	51.172	50.937	50.716	50.510	50.322	50.152	49.999	49.861	49.737	49.626	49.526	49.436	49.353	49.279	49.211	49.149	49.092	49.039	48.991
3	26.434	24.357	20.953	14.231	8.592	5.703	4.251	3.439	2.937	2.601	2.363	2.186	2.051	1.944	1.857	1.786	1.726	1.675	1.632
4	0.304	1.149	4.214	10.591	15.904	18.490	19.663	20.222	20.496	20.624	20.675	20.683	20.667	20.637	20.599	20.559	20.517	20.476	20.436
5	0.124	0.009	0.001	0.010	0.020	0.029	0.037	0.043	0.049	0.055	0.061	0.068	0.076	0.087	0.103	0.126	0.164	0.235	0.400
6	0.003	0.004	0.005	0.007	0.010	0.016	0.029	0.070	0.276	1.381	2.017	2.025	1.933	1.825	1.720	1.620	1.524	1.426	1.301
7	6.933	6.352	5.725	5.109	4.555	4.068	3.648	3.285	2.874	2.154	8.695	8.622	8.659	8.704	8.738	8.758	8.758	8.729	8.633
8	2.541	3.816	4.452	5.298	6.014	6.604	7.072	7.421	7.623	7.216	0.000	0.014	0.010	0.007	0.005	0.004	0.003	0.002	0.002
9	0.001	0.000	0.008	0.030	0.090	0.331	2.842	4.495	4.736	4.875	4.979	5.058	5.117	5.159	5.187	5.203	5.208	5.205	5.193
10	2.382	2.839	3.252	3.545	3.791	3.820	1.536	0.083	0.017	0.004	0.001	0.000	0.001	0.004	0.008	0.014	0.020	0.029	0.041
Total MMPR value for the first 10 modes ∑	89.970	89.496	89.336	89.332	89.299	89.218	89.089	88.939	88.771	88.569	88.356	88.137	87.919	87.702	87.488	87.281	87.080	86.886	86.701
11	0.076	0.075	0.055	0.034	0.016	0.003	0.004	0.005	0.006	0.030	0.061	0.097	0.138	0.188	0.249	0.330	0.439	0.598	0.838
12	0.177	1.001	0.904	0.950	1.058	1.271	1.572	1.890	2.155	2.355	2.504	2.616	2.698	2.753	2.781	2.780	2.745	2.670	2.244
13	0.011	0.012	0.016	0.028	0.207	1.063	0.812	0.520	0.371	0.294	0.249	0.217	0.192	0.170	0.149	0.127	0.099	0.050	0.265
14	0.000	0.134	0.884	1.059	0.949	0.034	0.109	0.203	0.202	0.184	0.178	0.191	0.224	0.288	0.405	0.634	1.074	1.667	1.994
15	0.636	0.370	0.074	0.054	0.021	0.000	0.000	0.000	0.001	0.002	0.003	0.005	0.008	0.016	0.034	0.083	0.064	0.017	0.209
16	0.122	0.231	0.185	0.061	0.000	0.499	1.406	1.586	1.638	1.639	1.611	1.568	1.511	1.433	1.327	1.294	1.198	0.703	0.246
17	0.040	0.036	1.382	1.495	1.575	0.999	0.000	0.011	0.052	0.121	0.205	0.291	0.372	0.441	0.472	0.287	0.019	0.022	0.012
18	0.094	0.006	0.006	0.121	0.090	0.172	0.278	0.113	0.051	0.015	0.010	0.574	0.800	0.908	0.983	1.047	1.105	1.160	1.211
19	0.001	0.000	0.023	0.000	0.001	0.001	0.005	0.011	0.024	0.059	0.208	0.195	0.114	0.085	0.077	0.074	0.072	0.072	0.072
20	1.347	1.315	0.098	0.012	0.000	0.000	0.046	0.370	0.785	0.826	0.653	0.001	0.036	0.040	0.046	0.060	0.086	0.133	0.219
Total MMPR value for the first 20 modes ∑	92.474	92.676	92.962	93.147	93.216	93.258	93.322	93.650	94.056	94.093	94.038	93.891	94.012	94.024	94.013	93.996	93.980	93.979	94.011
21	0.135	0.152	0.046	0.001	0.000	0.010	0.006	0.457	0.058	0.016	0.061	0.191	0.048	0.010	0.007	0.544	0.705	0.724	0.695
22	0.050	0.063	0.039	0.000	0.001	0.126	0.777	0.014	0.005	0.002	0.001	0.000	0.000	0.000	0.001	0.000	0.013	0.022	0.013
23	0.002	0.001	0.002	0.004	0.008	0.185	0.002	0.000	0.000	0.477	0.531	0.579	0.625	0.666	0.686	0.142	0.018	0.007	0.004
24	0.007	0.003	0.101	0.762	0.786	0.556	0.066	0.263	0.410	0.000	0.062	0.062	0.062	0.060	0.060	0.084	0.041	0.012	0.002
25	0.003	0.000	0.037	0.118	0.114	0.012	0.003	0.025	0.058	0.061	0.000	0.000	0.004	0.011	0.395	0.523	0.535	0.536	0.535
26	0.001	0.435	0.275	0.109	0.025	0.153	0.232	0.095	0.029	0.040	0.023	0.014	0.000	0.628	0.202	0.084	0.111	0.135	0.156
27	0.032	0.286	0.493	0.000	0.096	0.049	0.037	0.041	0.002	0.007	0.363	0.531	0.604	0.001	0.064	0.071	0.047	0.036	0.030
28	0.589	0.056	0.010	0.001	0.000	0.052	0.053	0.032	0.015	0.001	0.017	0.011	0.002	0.000	0.000	0.020	0.053	0.095	0.138
29	0.006	0.000	0.003	0.004	0.008	0.000	0.008	0.002	0.001	0.082	0.022	0.115	0.068	0.015	0.001	0.000	0.000	0.003	0.046
30	0.106	0.000	0.002	0.005	0.001	0.007	0.000	0.511	0.526	0.368	0.245	0.007	0.001	0.001	0.000	0.000	0.036	0.044	0.001
Total MMPR value for the first 30 modes ∑	93.405	93.674	93.970	94.151	94.254	94.408	94.506	95.089	95.161	95.147	95.364	95.402	95.425	95.417	95.428	95.464	95.539	95.593	95.630
31	0.003	0.001	0.116	0.000	0.019	0.000	0.490	0.001	0.091	0.168	0.001	0.000	0.000	0.019	0.018	0.000	0.011	0.206	0.193
32	0.029	0.111	0.003	0.000	0.000	0.063	0.031	0.083	0.000	0.000	0.000	0.000	0.004	0.019	0.051	0.045	0.122	0.000	0.000
33	0.091	0.210	0.005	0.007	0.006	0.019	0.041	0.000	0.000	0.000	0.037	0.015	0.002	0.173	0.308	0.307	0.147	0.021	0.000
34	0.152	0.022	0.011	0.005	0.503	0.420	0.003	0.000	0.091	0.063	0.000	0.000	0.344	0.174	0.037	0.174	0.216	0.250	0.273
35	0.276	0.031	0.000	0.010	0.062	0.074	0.016	0.052	0.000	0.000	0.063	0.074	0.037	0.016	0.005	0.011	0.029	0.029	0.029
36	0.003	0.022	0.013	0.021	0.009	0.001	0.000	0.002	0.000	0.172	0.362	0.320	0.000	0.000	0.099	0.012	0.058	0.046	0.032
37	0.000	0.008	0.002	0.282	0.000	0.006	0.108	0.062	0.000	0.040	0.000	0.038	0.060	0.086	0.000	0.004	0.011	0.003	0.005
38	0.066	0.020	0.000	0.048	0.021	0.010	0.002	0.001	0.051	0.063	0.010	0.000	0.113	0.098	0.015	0.098	0.000	0.000	0.126
39	0.025	0.015	0.009	0.108	0.024	0.002	0.005	0.002	0.054	0.013	0.000	0.087	0.034	0.057	0.128	0.000	0.000	0.000	0.000
40	0.006	0.015	0.015	0.063	0.002	0.000	0.001	0.000	0.013	0.154	0.002	0.027	0.000	0.000	0.002	0.008	0.032	0.116	0.242
Total MMPR value for the first 40 modes ∑	94.056	94.131	94.146	94.694	94.900	95.003	95.205	95.291	95.461	95.819	95.838	95.962	96.018	96.060	96.092	96.122	96.165	96.264	96.532
41	0.025	0.210	0.527	0.113	0.000	0.013	0.012	0.000	0.000	0.000	0.026	0.001	0.000	0.006	0.308	0.345	0.334	0.254	0.004
42	0.005	0.001	0.001	0.001	0.011	0.006	0.001	0.055	0.022	0.009	0.000	0.000	0.067	0.211	0.008	0.020	0.016	0.012	0.003
43	0.001	0.000	0.002	0.063	0.062	0.080	0.000	0.001	0.034	0.001	0.053	0.000	0.000	0.001	0.020	0.000	0.000	0.002	0.009
44	0.091	0.000	0.000	0.001	0.014	0.274	0.215	0.142	0.261	0.031	0.001	0.068	0.071	0.076	0.036	0.001	0.011	0.000	0.028
45	0.030	0.111	0.167	0.000	0.285	0.017	0.048	0.053	0.036	0.023	0.033	0.001	0.005	0.000	0.006	0.029	0.000	0.029	0.003
46	0.003	0.011	0.074	0.050	0.008	0.014	0.005	0.170	0.036	0.001	0.011	0.022	0.005	0.009	0.005	0.000	0.021	0.001	0.035
47	0.013	0.402	0.012	0.053	0.055	0.025	0.000	0.002	0.001	0.011	0.004	0.002	0.005	0.032	0.000	0.000	0.001	0.018	0.205
48	0.085	0.002	0.015	0.173	0.000	0.000	0.093	0.003	0.000	0.008	0.013	0.009	0.109	0.005	0.009	0.011	0.000	0.000	0.002
49	0.527	0.020	0.014	0.080	0.076	0.072	0.040	0.113	0.007	0.001	0.001	0.017	0.032	0.000	0.000	0.017	0.051	0.144	0.000
50	0.024	0.038	0.002	0.016	0.021	0.001	0.157	0.002	0.000	0.001	0.005	0.119	0.001	0.032	0.000	0.000	0.007	0.002	0.007
Total MMPR value for the first 50 modes ∑	94.859	94.925	94.961	95.244	95.432	95.507	95.775	95.833	95.858	95.904	95.986	96.200	96.314	96.432	96.484	96.545	96.607	96.727	96.827

Table 4. Modal mass participation ratios (MMPR) for the *y* direction.

Mode	α parameter values (m)																			
	6.0	6.5	7.0	7.5	8.0	8.5	9.0	9.5	10.0	10.5	11.0	11.5	12.0	12.5	13.0	13.5	14.0	14.5	15.0
1	51.066	50.880	50.700	50.531	50.373	50.228	50.095	49.974	49.863	49.762	49.670	49.586	49.508	49.437	49.372	49.311	49.256	49.204	49.155
2	0.079	0.033	0.010	0.001	0.001	0.005	0.012	0.019	0.027	0.034	0.041	0.047	0.053	0.058	0.062	0.066	0.069	0.072	0.075
3	0.220	0.978	3.761	9.664	14.682	17.203	18.409	19.034	19.383	19.590	19.715	19.792	19.840	19.869	19.886	19.894	19.897	19.896	19.893
4	23.433	22.513	19.517	13.410	8.203	5.511	4.151	3.387	2.913	2.594	2.369	2.200	2.071	1.968	1.884	1.815	1.757	1.707	1.665
5	0.140	0.047	0.023	0.014	0.009	0.007	0.005	0.004	0.003	0.003	0.002	0.002	0.002	0.002	0.002	0.002	0.002	0.002	0.000
6	0.000	0.001	0.005	0.013	0.028	0.057	0.124	0.320	1.220	5.274	7.578	8.084	8.302	8.439	8.540	8.620	8.687	8.750	8.821
7	2.635	3.585	4.468	5.246	5.889	6.400	6.767	6.901	6.216	2.019	1.683	1.872	1.799	1.702	1.607	1.517	1.433	1.349	1.256
8	7.242	6.456	5.690	4.988	4.388	3.883	3.467	3.141	2.921	3.050	1.064	0.346	0.174	0.106	0.072	0.053	0.040	0.032	0.026
9	0.000	0.001	0.005	0.015	0.044	0.148	0.369	0.125	0.061	0.033	0.018	0.009	0.003	0.001	0.000	0.001	0.005	0.010	0.018
10	0.411	0.309	0.212	0.133	0.067	0.008	0.030	0.502	0.784	0.964	1.042	1.084	1.109	1.121	1.126	1.123	1.116	1.104	1.087
Total MMPR value for the first 10 modes ∑	85.225	84.801	84.391	84.015	83.684	83.450	83.427	83.406	83.391	83.324	83.182	83.022	82.862	82.704	82.550	82.403	82.261	82.125	81.996
11	3.896	4.171	4.405	4.589	4.723	4.758	4.580	3.905	0.227	0.105	0.064	0.046	0.037	0.033	0.030	0.031	0.033	0.037	0.045
12	0.141	0.128	0.133	0.150	0.181	0.220	0.256	0.271	0.265	0.248	0.228	0.208	0.189	0.169	0.148	0.124	0.093	0.041	0.366
13	0.079	0.081	0.089	0.110	0.192	0.353	1.137	1.903	2.251	2.417	2.515	2.583	2.633	2.674	2.710	2.744	2.781	2.833	2.505
14	0.002	0.017	0.015	0.002	0.000	0.467	1.298	1.064	0.251	0.127	0.072	0.043	0.027	0.016	0.007	0.001	0.008	0.082	0.240
15	0.053	0.176	2.142	2.220	2.195	1.598	0.006	0.009	0.022	0.033	0.045	0.061	0.087	0.142	0.282	0.721	1.598	2.186	2.237
16	0.862	1.840	0.001	0.000	0.000	0.008	0.005	0.004	0.046	0.128	0.231	0.338	0.437	0.511	0.500	0.150	0.234	0.080	0.003
17	0.119	0.006	0.217	0.198	0.158	0.313	1.987	2.057	2.076	2.048	1.992	1.921	1.842	1.758	1.668	1.614	0.671	0.187	0.075
18	0.832	0.026	0.001	1.513	1.665	1.593	0.000	0.000	0.000	0.001	0.025	0.066	0.057	0.052	0.051	0.052	0.053	0.055	0.056
19	0.044	0.022	0.003	0.014	0.016	0.006	0.001	0.000	0.003	0.014	0.028	0.504	1.206	1.353	1.415	1.455	1.486	1.513	1.537
20	0.242	0.229	0.976	0.035	0.010	0.008	0.278	0.512	0.129	0.073	0.271	0.825	0.190	0.079	0.049	0.037	0.032	0.032	0.034
Total MMPR value for the first 20 modes ∑	91.495	91.496	92.372	92.846	92.823	92.774	92.975	93.131	92.662	92.518	92.653	93.618	93.568	93.490	93.410	93.330	93.249	93.171	93.093
21	1.026	1.182	0.401	0.000	0.000	0.090	0.008	0.417	1.123	1.253	1.061	0.024	0.000	0.000	0.001	0.039	0.048	0.036	0.015
22	0.062	0.080	0.063	0.001	0.006	0.008	0.010	0.373	0.073	0.017	0.003	0.000	0.001	0.007	0.026	0.132	0.582	0.879	0.973
23	0.003	0.013	0.023	0.039	0.073	0.586	0.978	0.004	0.003	0.092	0.095	0.096	0.095	0.092	0.089	0.094	0.339	0.081	0.032
24	0.002	0.000	0.001	0.150	0.140	0.238	0.017	0.057	0.083	0.006	0.655	0.699	0.739	0.774	0.792	0.675	0.000	0.000	0.000
25	0.005	0.000	0.039	1.037	1.046	0.362	0.028	0.113	0.544	0.603	0.002	0.001	0.003	0.012	0.051	0.094	0.138	0.174	0.204
26	0.041	0.232	0.614	0.000	0.001	0.032	0.048	0.035	0.005	0.002	0.001	0.002	0.001	0.000	0.457	0.760	0.735	0.714	0.699
27	0.007	0.226	0.431	0.001	0.009	0.004	0.402	0.373	0.014	0.004	0.030	0.020	0.005	0.811	0.333	0.004	0.001	0.000	0.000
28	0.096	0.183	0.001	0.000	0.002	0.320	0.011	0.002	0.000	0.004	0.688	0.761	0.797	0.001	0.001	0.007	0.013	0.020	0.026
29	0.017	0.289	0.014	0.001	0.026	0.003	0.000	0.000	0.002	0.008	0.041	0.000	0.000	0.000	0.003	0.000	0.000	0.026	0.452
30	0.647	0.005	0.004	0.000	0.005	0.001	0.003	0.100	0.108	0.203	0.000	0.001	0.000	0.000	0.000	0.000	0.317	0.420	0.006
Total MMPR value for the first 30 modes ∑	93.400	93.706	93.961	94.077	94.132	94.417	94.480	94.604	94.617	94.709	95.230	95.223	95.209	95.188	95.163	95.136	95.424	95.521	95.500
31	0.001	0.003	0.032	0.005	0.151	0.002	0.095	0.001	0.580	0.513	0.001	0.000	0.001	0.001	0.001	0.022	0.102	0.037	0.031
32	0.003	0.024	0.009	0.002	0.000	0.003	0.134	0.549	0.008	0.002	0.001	0.003	0.001	0.333	0.424	0.422	0.061	0.001	0.002
33	0.251	0.055	0.002	0.000	0.001	0.014	0.347	0.002	0.000	0.005	0.003	0.001	0.010	0.001	0.040	0.031	0.000	0.001	0.000
34	0.083	0.237	0.135	0.027	0.098	0.088	0.009	0.006	0.010	0.007	0.004	0.003	0.030	0.036	0.009	0.037	0.039	0.039	0.037
35	0.051	0.018	0.004	0.001	0.406	0.448	0.012	0.008	0.003	0.000	0.408	0.408	0.438	0.113	0.025	0.073	0.322	0.344	0.362
36	0.024	0.092	0.000	0.320	0.064	0.008	0.011	0.002	0.001	0.003	0.058	0.068	0.006	0.004	0.029	0.161	0.003	0.002	0.001
37	0.007	0.000	0.000	0.016	0.050	0.000	0.009	0.006	0.000	0.308	0.011	0.020	0.024	0.028	0.004	0.073	0.001	0.000	0.002
38	0.147	0.032	0.016	0.257	0.000	0.002	0.000	0.000	0.011	0.002	0.015	0.001	0.022	0.047	0.266	0.004	0.002	0.003	0.241
39	0.049	0.000	0.002	0.002	0.004	0.053	0.000	0.001	0.000	0.113	0.000	0.014	0.193	0.204	0.002	0.003	0.003	0.001	0.003
40	0.000	0.114	0.437	0.075	0.006	0.002	0.040	0.021	0.000	0.009	0.000	0.147	0.002	0.000	0.012	0.030	0.086	0.204	0.165
Total MMPR value for the first 40 modes ∑	94.016	94.282	94.598	94.783	94.913	95.038	95.138	95.200	95.232	95.670	95.731	95.888	95.933	95.955	95.974	95.993	96.043	96.153	96.344
41	0.001	0.008	0.016	0.002	0.005	0.001	0.008	0.001	0.000	0.162	0.002	0.002	0.148	0.057	0.016	0.033	0.050	0.150	0.027
42	0.006	0.004	0.013	0.008	0.001	0.000	0.016	0.001	0.024	0.010	0.139	0.011	0.002	0.027	0.072	0.403	0.323	0.102	0.022
43	0.488	0.000	0.001	0.006	0.008	0.012	0.000	0.068	0.417	0.021	0.000	0.129	0.014	0.225	0.384	0.000	0.001	0.000	0.001
44	0.002	0.459	0.340	0.011	0.028	0.046	0.045	0.037	0.059	0.000	0.004	0.001	0.000	0.001	0.003	0.006	0.000	0.001	0.005
45	0.012	0.017	0.031	0.273	0.038	0.195	0.395	0.431	0.113	0.001	0.004	0.007	0.008	0.006	0.011	0.001	0.000	0.004	0.037
46	0.033	0.006	0.004	0.006	0.110	0.159	0.016	0.014	0.002	0.002	0.070	0.000	0.004	0.034	0.001	0.057	0.002	0.013	0.220
47	0.026	0.070	0.007	0.014	0.317	0.082	0.018	0.004	0.001	0.002	0.011	0.001	0.006	0.098	0.003	0.006	0.125	0.251	0.035
48	0.081	0.014	0.002	0.063	0.202	0.203	0.002	0.002	0.001	0.039	0.032	0.020	0.038	0.002	0.002	0.000	0.009	0.005	0.001
49	0.034	0.078	0.126	0.285	0.018	0.004	0.006	0.017	0.000	0.002	0.003	0.015	0.128	0.014	0.000	0.000	0.000	0.016	0.002
50	0.003	0.089	0.077	0.009	0.015	0.012	0.121	0.038	0.000	0.001	0.001	0.023	0.001	0.009	0.000	0.000	0.128	0.008	0.057
Total MMPR value for the first 50 modes ∑	94.703	95.027	95.214	95.461	95.655	95.754	95.764	95.814	95.849	95.911	95.995	96.097	96.281	96.428	96.467	96.499	96.681	96.703	96.750

- It has been determined that the natural frequency values decrease as the minaret height increases (in case of the *a* parameter increases from 6.0 to 15.0). However, this amount of decrease did not occur proportionally between the increase in the natural frequency number and the increase in the height.
- Mode shapes are generally similar in the first modes. However, it has been observed that this similarity gradually decreases for the following modes.
- For the first 10 modes, it was determined that as the minaret height increased, the modal mass participation ratios in both *x* and *y* directions decreased.
- For the first 10 modes, a modal mass participation ratios of over 80% was achieved in both directions (*x*-*y*). These ratios were higher in the *x* direction and ranged from 86.701 to 89.970%. In the *y* direction, these ratios are in the range of 81.996-85.225%.
- For the first 20 and 30 modes, no linear relationship could be obtained between the change in minaret height and the change in modal mass participation ratios.
- For the first 40 and 50 modes, it has been determined that as the minaret height increases, the modal mass participation ratios increase in both *x* and *y* directions.

In the study, an equation was derived that allows the first natural frequency of minarets to be estimated depending on the minaret height. It should be noted that this equation is specific to the selected minaret material and geometry properties. It will be useful to develop this equation for minarets with different material and geometry properties.

Acknowledgements

None declared.

Funding

The authors received no financial support for the research, authorship, and/or publication of this manuscript.

Conflict of Interest

The authors declared no potential conflicts of interest with respect to the research, authorship, and/or publication of this manuscript.

References

Adam MA, El-Salakawy TS, Salama MA, Mohamed AA (2020). Assessment of structural condition of a historic masonry minaret in Egypt. *Case Studies in Construction Materials,* 13, e00409.

ANSYS Inc. (2017). ANSYS Mechanical Theory Reference: Release 18.1. Canonsburg, PA, USA.

Bayraktar A, Hökelekli E (2020). Influences of earthquake input models on nonlinear seismic performances of minaret-foundation-soil interaction systems. *Soil Dynamics and Earthquake Engineering,* 139, 106368.

Bayraktar A. Hökelekli E (2021). A cost-effective FRCM technique for seismic strengthening of minarets. *Engineering Structures,* 229, 111672.

Calayır Y, Yetkin M, Erkek H (2021). Finite element model updating of masonry minarets by using operational modal analysis method. *Structures,* 34, 3501-3507.

MPDG (2021). Cami Planlama ve Tasarımı Kılavuzu, Presidency of the Republic of Türkiye Presidency of Religious Affairs, Ankara, Türkiye (in Turkish).

Döven M, Serhatoğlu C, Kaplan O, Livaoğlu R (2018). Dynamic behavior change of Kütahya Yeşil Minaret with covered and open balcony architecture. *Eskişehir Technical University Journal of Science and Technology B- Theoritical Sciences,* 6, 192–203 (in Turkish).

Köksal O, Hacıefendioğlu K, Alpaslan E, Birinci F (2016). Influence of blast-induced ground motion on dynamic response of masonry minaret of Yörgüç Paşa Mosque. *Challenge Journal of Structural Mechanics,* 3(1), 31–37.

Usta P (2021). Assessment of seismic behavior of historic masonry minarets in Antalya, Türkiye. *Case Studies in Construction Materials,* 15, e00665.

Yetkin M, Erkek H, Calayır Y (2018). Determining dynamic characteristics of reinforced concrete minarets and updating of their finite element models using environmental vibration data. *Fırat University Turkish Journal of Science & Technology,* 13(1), 93-98.

Yetkin M, Dedeoğlu İÖ, Calayır Y (2021a). Investigation and assessment of damages in the minarets existing at Elazig after 24 January 2020 Sivrice Earthquake. *Fırat University Journal of Engineering Science,* 33(2), 379-389 (in Turkish).

Yetkin M, Erkek H, Calayır Y (2021b). Model updating of a reinforced concrete minaret by using ambient vibration tests. *9th Turkish Conference on Earthquake Engineering*, Istanbul, Türkiye, 459-467.

Yetkin M, Erkek H, Calayır, Y (2021c). Comparison of measurements with and without reference in operational modal analysis method: A minaret example. *Journal of the Institute of Science and Technology,* 11(3), 2069-2078 (in Turkish).

Yurdakul M, Yılmaz F, Artar M, Can Ö, Öner E, Daloğlu AT (2021). Investigation of time-history response of a historical masonry minaret under seismic loads. *Structures,* 30, 265-276.